



## New relative sea-level insights into the isostatic history of the Western Mediterranean

Matteo Vacchi <sup>a, b, \*</sup>, Matthieu Ghilardi <sup>c</sup>, Rita T. Melis <sup>d</sup>, Giorgio Spada <sup>e</sup>,  
Matthieu Giaime <sup>f</sup>, Nick Marriner <sup>g</sup>, Thomas Lorscheid <sup>h</sup>, Christophe Morhange <sup>c, l</sup>,  
Francesc Burjachs <sup>i, j, k</sup>, Alessio Rovere <sup>h</sup>

<sup>a</sup> Geography, College of Life and Environmental Sciences, University of Exeter, EX4 4RJ, Exeter, UK

<sup>b</sup> Dipartimento di Scienze Della Terra, Università di Pisa, Via S. Maria, 53, 56126, Pisa, Italy

<sup>c</sup> Aix-Marseille Université, CNRS-CEREGE, UMR 7330, IRD, Collège de France, INRA Aix en Provence, France

<sup>d</sup> Dipartimento Scienze Chimiche e Geologiche, Università Degli Studi di Cagliari, Via Trentino 51, 09127, Cagliari, Italy

<sup>e</sup> Università Degli Studi di Urbino, Dipartimento di Scienze Pure e Applicate (DiSPeA), Urbino, Italy

<sup>f</sup> Department of Geography, Durham University, South Road, Durham, DH1 3LE, UK

<sup>g</sup> CNRS Chrono-Environnement UMR6249, Université de Franche-Comté, UFR ST, Besancon, France

<sup>h</sup> University of Bremen, Marum, ZMT, D-28359, Bremen, Germany

<sup>i</sup> ICREA, Barcelona, Catalonia, Spain

<sup>j</sup> IPHES, Institut Català de Paleocologia Humana i Evolució Social, Campus Sescelades URV, Tarragona, Catalonia, Spain

<sup>k</sup> URV, Àrea de Prehistòria, Universitat Rovira i Virgili, 43002, Tarragona, Catalonia, Spain

<sup>l</sup> RIMS, The Leon Recanati Institute for Maritime Studies University of Haifa, Mount Carmel, Haifa 31905, Israel

### ARTICLE INFO

#### Article history:

Received 15 January 2018

Received in revised form

16 October 2018

Accepted 17 October 2018

#### Keywords:

Sea-level changes

Isostatic adjustment

Vertical crustal motion

Holocene

Mediterranean sea

### ABSTRACT

A recent suite of Relative Sea-Level (RSL) data for the past 12 ka BP has provided new insights into the sea-level histories of the western Mediterranean region. Our analysis of the chronostratigraphic context of sea-level indicators from Spain (Catalonia, the Balearic Islands and the Gulf of Valencia), France (Corsica Island) and Italy (Sardinia Island) has yielded 162 new sea-level index and limiting points. These data have considerably enhanced previous RSL compilations, in addition to improving the quality of spatio-temporal sea-level reconstructions and our capacity to estimate isostatic-related vertical motions in the western Mediterranean basin. The glacial and hydro-isostatic adjustment (GIA) pattern elucidated by the new database shows discrepancy with respect to those predicted by the available GIA models. In particular, the new results underscore a non-coherent isostatic response of the central portion of the western Mediterranean, with the Balearic Islands manifesting significant departures from the sea-level histories of Corsica, Sardinia and, more generally, along most of the western Mediterranean coast. Our results are a crucial contribution to defining both the pattern and the magnitude of the isostatic signal along the western Mediterranean coast. In fact, vertical isostatic motions represent a key to better assess any possible post-industrial acceleration in sea-level rise and to define future scenarios of coastal inundation in the context of global change.

© 2018 Elsevier Ltd. All rights reserved.

### 1. Introduction

Understanding how changing ice volumes have contributed to sea-level rise in the past can provide insights into the sensitivity of ice sheets to future warmer conditions, and constrain physical

models used to project ice-sheet response to future climate change (e.g., Kopp et al., 2009; Dutton et al., 2015; Purcell et al., 2016). Glacial and hydro-isostatic adjustment (GIA) constitutes an important driver of past, present and future sea-level variability (e.g. Milne et al., 2009; Gehrels et al., 2011; Khan et al., 2015). For this reason, a major focus of current sea-level research is the continuous improvement of GIA geophysical models in an attempt to provide more accurate constraints for future sea-level scenarios (e.g. Nicholls et al., 2014; Goldberg et al., 2016; Roy and Peltier, 2018). Our understanding of current rates of sea-level rise from

\* Corresponding author. Geography, College of Life and Environmental Sciences, University of Exeter, EX4 4RJ, Exeter, UK.

E-mail address: [m.vacchi@exeter.ac.uk](mailto:m.vacchi@exeter.ac.uk) (M. Vacchi).

tide gauges or satellite data (e.g. Church and White, 2006; Cazenave et al., 2014; Bonaduce et al., 2016) requires correction for GIA effects that can be quantified using observations of former sea levels (e.g. Kemp et al., 2009; Engelhart et al., 2011; Rovere et al., 2016). Holocene (i.e. the last 12.0 ka BP) Relative Sea-Level (RSL) reconstructions have frequently been used to test and calibrate GIA models over timescales longer than the instrumental record (e.g., Shennan and Horton, 2002; Engelhart et al., 2011; Bradley et al., 2016; Edwards et al., 2017; Khan et al., 2017).

According to published geophysical models (e.g. Lambeck and Purcell, 2005; Stocchi and Spada, 2007, 2009; Lambeck et al., 2011; Roy and Peltier, 2018), GIA-related deformation in the Western Mediterranean is mainly controlled by water loading, which has resulted in widespread subsidence throughout much of the basin at an average rate of RSL rise of  $\sim 1 \text{ mm a}^{-1}$  over the last 6000 years. Such models were tuned with RSL data from several areas, particularly from the Italian coast (e.g., Lambeck et al., 2004, 2011; Antonioli et al., 2009) and the western Mediterranean (Vacchi et al., 2016). However, due to its complex tectonic setting (e.g., Ferranti et al., 2006; Faccenna et al., 2014), RSL histories from the Mediterranean Sea are often reported as being influenced by the Holocene activity of major faults (e.g., Stiros et al., 2000; Mastronuzzi and Sansò, 2002; Scicchitano et al., 2011). This has often hampered the identification of the GIA component in the RSL record. This issue is even more complex in those coastal regions located at the mouth of major Mediterranean rivers (e.g., Amorosi et al., 1999, 2013; Vella et al., 2005; Marriner et al., 2012a), where the RSL record is strongly affected by long-term subsidence induced by sediment loading and compaction.

The aim of this study is to improve the quality of spatio-temporal sea-level reconstructions along a large portion of the Mediterranean coast of Spain (Catalonia coast, the Balearic Islands

and the Gulf of Valencia, Fig. 1), Corsica (France) and Sardinia (Italy), the third and second largest islands of the western Mediterranean Sea, respectively (Fig. 1). These regions are generally located far from major tectonic boundaries (e.g. much of the northern Spanish Mediterranean coast, Fig. 1). Furthermore, Balearic, Corsica and Sardinia Islands are located in the centre of the basin, where GIA models predict a maximum hydro-isostatic contribution (e.g., Lambeck and Purcell, 2005; Stocchi and Spada, 2009; Roy and Peltier, 2018). In all five regions, conflicting sea-level histories (see section 3), in addition to poor data quality or a paucity of Sea Level Index Points (SLIPs, Shennan et al., 2015), have hindered the construction of robust RSL histories and, as a result, a clear understanding of the isostatic contribution (Vacchi et al., 2016). However, a significant number of new studies has been published since 2016 for these regions (see section 3). We critically reviewed these recently published studies that, along with older data, allowed us to produce a new suite of SLIPs and RSL limiting points following the protocol described by the International Geoscience Programme (IGCP) projects 61, 200, 495 and 588 (e.g., Preuss, 1979; van de Plassche, 1982; Gehrels and Long, 2007; Shennan et al., 2015). We subsequently compared the reconstructed RSL histories with the predictions based on the ICE-6G (VM5a) GIA model (Peltier et al., 2015) to visualize and discuss the spatio-temporal variability of the isostatic response in the Western Mediterranean.

## 2. Study area

The study area encompasses a large portion of the Western Mediterranean basin, at latitudes between  $\sim 39.0^\circ \text{ N}$  and  $\sim 43.0^\circ \text{ N}$  and longitudes between  $\sim -0.5^\circ \text{ E}$  and  $\sim 10^\circ \text{ E}$  (Fig. 1). The area is characterized by a microtidal regime, with tidal ranges typically not exceeding 0.45 m (Tsimplis et al., 1995).

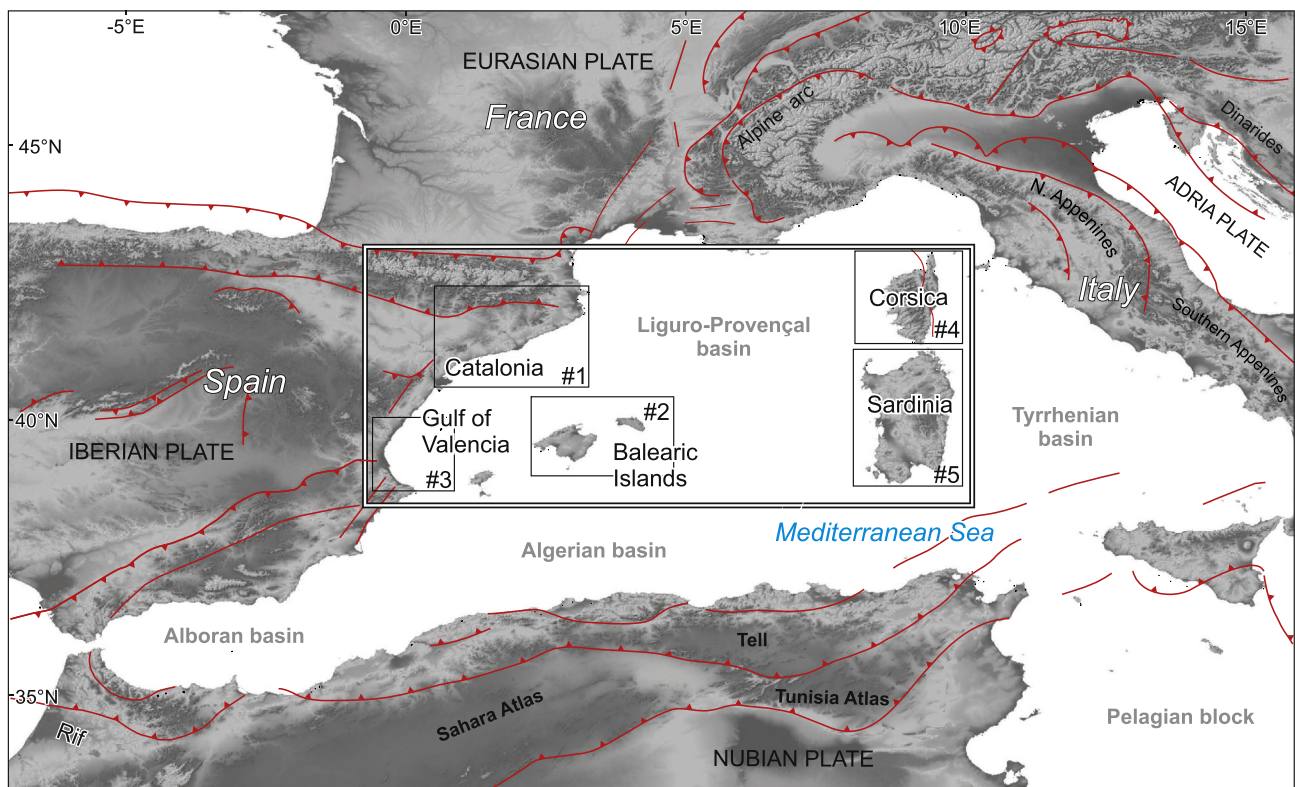


**Fig. 1.** Spatial extent of the study area. Numbered rectangles denote the location of sea-level data for this study, grouped into five regions as explained in the text. Tectonic framework of the western Mediterranean. Faults are modified after Faccenna et al. (2014) and Vacchi et al. (2016).

The long record of historical seismicity, coupled with on-going crustal deformation, contributed to define the neotectonic framework of the Western Mediterranean (e.g. Faccenna et al., 2014; Serpelloni et al., 2007; Nocquet, 2012). Two small oceanic basins (the Tyrrhenian and the Liguro-Provençal back-arc basins) lie on the Nubia-Eurasia convergent margin and are separated by the Corsica-Sardinia rigid continental block (e.g. Vernant et al., 2010; Faccenna et al., 2014). Some parts of the back-arc basin margins are undergoing active compressional tectonics along the east-Alboran, Algerian, and south-Tyrrhenian margins (Billi et al., 2011; Serpelloni et al., 2013). The south-Tyrrhenian compressional domain extends to northeast Sicily, while the Tyrrhenian side of the Calabrian Arc and central-southern Apennines are dominated by extension (Fig. 1; e.g., Ferranti et al., 2006; Faccenna et al., 2014). In these coastal areas, a major tectonic influence on the Holocene RSL evolution has often been reported (e.g., Ferranti et al., 2010; Scicchitano et al., 2011). By contrast, tectonic stability characterizes much of the Tyrrhenian and Liguro-Provençal basin (e.g. Ferranti et al., 2006; Billi et al., 2011; Nocquet, 2012). All of the coastal sectors discussed in this paper lie within areas characterized by a minimal or negligible tectonic influence on the late-Quaternary RSL evolution (e.g., Ferranti et al., 2006; Lorscheid et al., 2017; Stocchi et al., 2018). Absence of historical seismicity characterizes much of the Spanish regions included in the database (regions 1, 2 and 3, Fig. 1). One possible exception is the Valencia coastal plain, where weak seismic activity (<5.0 M) is reported (Olivera et al., 1992; Anzidei et al., 2014). Both Corsica (France) and Sardinia (Italy) (regions 4 and 5, Fig. 1) are widely acknowledged to be amongst the most tectonically stable areas of the Mediterranean, with the absence of significant historical seismicity (Nocquet, 2012). In addition, Ferranti et al. (2006) defined negligible vertical motions during the last ~ 125 ka BP according to the present elevation of the last interglacial shoreline.

### 3. Previous sea-level compilations and recent sources of the RSL datapoints

A review of the available RSL data at the Western Mediterranean scale (Vacchi et al., 2016) allowed us to constrain coastal areas where Holocene RSL histories were conflicting, of low quality or almost non-existent. For the Catalonia coast, extending along the northernmost portion of the Spanish Mediterranean coast (region 1, Fig. 1), previous data included beachrock samples and lagoonal data, the current positions of which have been significantly affected by sediment compaction, especially during the mid to late-Holocene (Somoza et al., 1998; Roqué Pau and Pallí Buxó, 1997; Gámez Torrent, 2007; Vacchi et al., 2016). Recent investigations on the Barcelona and Empúries coastal plains (Daura et al., 2016; Ejarque et al., 2016), in the Ebro Delta (Cearreta et al., 2016) and on remains of seagrass palaeo-soils (*Posidonia oceanica* mats, López-Merino et al., 2017) provided useful new data to help to evaluate the RSL history of the area. The Vacchi et al. (2016) review did not include a Holocene RSL curve for the Balearic Islands (region 2, Fig. 1). This was mainly due to the very limited amount of RSL data in the area. However, recent investigations performed in Mallorca and Menorca (Burjachs et al., 2017; Giaime et al., 2017) coupled with the sparse older data (Fornós et al., 1998; Yll et al., 1999) allowed us to comprehensively reassess the RSL history of this insular complex.

Vacchi et al. (2016) underlined the poor quality of the RSL reconstruction for the Gulf of Valencia (region 3, Fig. 1). Large uncertainties are associated with the SLIPs and poor descriptions of the original data did not allow us to robustly assess the RSL history in this area, notably for the last 6000 years. A new dataset of dated estuarine facies (Carmona et al., 2016; Blázquez et al., 2017;

Rodríguez-Pérez et al., 2018) has facilitated a significant advance in the definition of the mid-to late-Holocene RSL evolution of this coastal sector.

RSL histories in Corsica (region 4) show some inconsistencies (Vacchi et al., 2016). Fossil fixed biological indicators sampled on the northern coast of the island (Laborel et al., 1994) indicate that RSL variations during the last ~4.0 ka BP did not exceed ~2 m (Vacchi et al., 2016); these data are in agreement with the new RSL dataset produced by Vacchi et al. (2017) for the eastern coast of Corsica. Conversely, data obtained from a series of submerged beachrocks in the Bonifacio Strait (i.e. the narrow strait dividing Corsica and Sardinia, see Fig. 4, Nesteroff, 1984; De Muro and Orrù, 1998; Lambeck et al., 2004) show a significant departure from the above-mentioned data, with an offset of up to -3 m, especially for the mid to late-Holocene (Vacchi et al., 2017). Such a discrepancy is difficult to explain in terms of the tectonic setting (see section 2) or compaction-related subsidence (Vacchi et al., 2016). In this database, we tried to resolve these discrepancies by including a new RSL dataset derived from palaeoenvironmental investigations recently performed in several Corsican coastal marshes and lagoons (Currás et al., 2017; Ghilardi et al., 2017a; b; Poher et al., 2017; Vacchi et al., 2017).

Sardinia (region 5) has been widely investigated and several types of sea-level data have been used to infer the RSL evolution (De Muro and Orrù, 1998; Orrù et al., 2004, 2011; 2014; Pirazzoli, 2005; Antonioli et al., 2007, 2012; De Falco et al., 2015). These data mainly constrain the late-Holocene RSL evolution. Conversely, a larger scatter is present in the early to mid-Holocene data. This is essentially related to compaction (such as in the Cagliari coastal plain, Antonioli et al., 2007) or beachrock dating problems (Vacchi et al., 2016, 2017). Sardinia has also been the object of recent investigations (Melis et al., 2017, 2018; Palombo et al., 2017; Pascucci et al., 2018; Ruiz et al., 2018), mainly focused on multiproxy palaeoenvironmental reconstructions, yielding new sea-level data in these coastal areas.

### 4. Production of RSL datapoints

#### 4.1. RSL index and limiting points

Most of the SLIPs (cf. Shennan et al., 2015; Hijma et al., 2015) in the database are derived from cores in coastal and alluvial plains, coastal marshes and lagoons. In particular, lagoons (i.e. low-energy inland waterbodies that are either intermittently or continuously connected to the open sea) are very common geomorphological features on clastic Mediterranean coasts (e.g., Di Rita et al., 2011; Salel et al., 2016; Fontana et al., 2017). Here, water depth very seldom exceeds a few meters (e.g., Marco-Barba et al., 2013; Di Rita and Melis, 2013) and samples collected in lagoonal facies have often been used to assess the palaeo sea-level position (e.g., Primavera et al., 2011; Sander et al., 2015, 2016; Vacchi et al., 2017).

In this study, we produced SLIPs from sedimentary records following the recent protocol developed for the Mediterranean (Vacchi et al., 2016, Table 1). This methodology has recently been applied to a number of studies focused on Mediterranean RSL reconstructions (e.g., Fontana et al., 2017; Karkani et al., 2017, 2018; Melis et al., 2017, 2018; Ruello et al., 2017; Vacchi et al., 2017; Ghilardi et al., 2018; Kaniewski et al., 2018). The definition of the depositional facies was based on biostratigraphy and, in particular, on the macro- and micro-faunal assemblages (i.e., malacofauna, foraminifera and ostracod assemblages, e.g., Morhange et al., 2001; Rossi et al., 2011; Marriner et al., 2012b, 2014). The detailed description of the indicative meaning associated with the different depositional facies (Table 1) is provided in Vacchi et al. (2016).

We subsequently added to the database beachrocks, fixed



**Table 1**

Summary of the indicative meanings used to estimate the relative elevation of the sea-level index points (SLIPs) and limiting points for the database (see Vacchi et al., 2016 for the detailed facies descriptions). HAT: Highest Astronomical Tide; MHW: Mean High Water; MLW: Mean Low Water; MSL: Mean Sea Level. Note that the investigated coastal sectors have a lower microtidal regime. HAT values are equivalent to the Mean Highest High Water and typically do not exceed 0.05 m above MHW. Similarly, the Mean Lowest Low Water values are equivalent to the MLW.

Sample Type	Evidence	Reference Water Level	Indicative Range
<b>SLIPs</b>			
<i>Lithophyllum byssoides</i> rim	Identifiable <i>in situ</i> coralline rhodophyte <i>Lithophyllum byssoides</i> (formerly known as <i>Lithophyllum lichenoides</i> ) recognized at species level (Laborel et al., 1994; Faivre et al., 2013).	(HAT to MSL)/2	HAT to MSL
Salt-marsh	Salt-marsh plant macrofossils (e.g. Vella et al., 2005; Di Rita et al., 2011; Primavera et al., 2011). Foraminiferal assemblages dominated by saltmarsh taxa (e.g., Caldara and Simone, 2005; Shaw et al., 2016; Cearreta et al., 2016).	(HAT to MSL)/2	HAT to MSL
Open or marine influenced lagoon	Macrofossil taxa dominated by marine brackish molluscs with the presence of <i>Cerastoderma glaucum</i> , <i>Bittium reticulatum</i> often associated with <i>Cerithium vulgatum</i> and <i>Loripes lacteus</i> (e.g. Di Rita et al., 2011; Giaime et al., 2017; Melis et al., 2018). Foraminiferal and ostracods assemblages dominated by marine brackish littoral taxa or outer estuary taxa (e.g., Marriner et al., 2012b; Carmona et al., 2016; Salel et al., 2016). Higher species diversity compared to the semi-enclosed lagoon system.	–1 m	MSL to –2 m
Inner or semi enclosed lagoon	Macrofossil taxa dominated by brackish molluscs typical of sheltered marine-lacustrine environments with the presence of <i>Cerastoderma glaucum</i> , <i>Abra segmentum</i> , Hydrobiidae spp. (e.g. Marriner et al., 2012b; Sabatier et al., 2012; Ghilardi et al., 2017a; b). Foraminifera and ostracod assemblages dominated by brackish littoral taxa or inner estuarine taxa (Ejarque et al., 2016; Salel et al., 2016, Cearreta et al., 2016). Lower species diversity compared to the open lagoon system.	–0.5 m	MSL to –1 m
Undifferentiated brackish environment	Foraminiferal, diatom and ostracod assemblages dominated by freshwater-slightly brackish or swamp taxa and shallow marine taxa (e.g. Amorosi et al., 2013; Ghilardi et al., 2017a; b).	(HAT to MLW)/2	HAT to MLW
Beachrock with cement fabric or stratigraphic information	Samples showing intergranular intertidal cements (i.e., irregularly distributed needles or isopachous fibres of aragonitic cement or isopachous rims (bladed or fibrous) and micritic High-Mg Calcite cement e.g. Vacchi et al., 2012; Mauz et al., 2015)	(HAT to MLW)/2	HAT to MLW
General beachrock	Samples that do not meet the above requirements for a classification as intertidal beachrocks (e.g., Vacchi et al., 2016)	0.5 m	–1 to +2 m MSL
<b>Limiting Points</b>			
Marine limiting	Identifiable marine shells in poorly to well-bedded sandy and silty sediments typical of the upper shoreface or prodelta environments (e.g., Morhange et al., 2011; Sabatier et al., 2012; Marriner et al., 2012b). <i>Posidonia oceanica</i> beds found in inner bay and shoreface marine deposits (Vacchi et al., 2017; Pascucci et al., 2018). Foraminiferal and ostracod assemblages dominated by marine taxa (Carboni et al., 2002; Rossi et al., 2011; Amorosi et al., 2013, Salel et al., 2016).	MSL	Below MSL
Terrestrial limiting	Freshwater plant macrofossils and peat with freshwater diatoms (e.g. Di Rita et al., 2010; Melis et al., 2017). Upper beach/foreshore deposits and terrestrial paleosoils. Foraminiferal and ostracod assemblages dominated by freshwater taxa in swamps or fluvial environments (Carboni et al., 2002; Rossi et al., 2011; Salel et al., 2016).	MSL	Above MSL

biological and archaeological SLIPs already present in previous RSL reconstructions for the area (Lambeck et al., 2011; Vacchi et al., 2016).

All samples that did not show a clear and robustly established relationship with the MSL were converted into limiting points (Engelhart et al., 2015; Vacchi et al., 2016). These data are extremely important in constraining the RSL position above or below a reconstructed elevation. Reconstructed RSL points must fall below terrestrial limiting points and above marine limiting points (e.g. Engelhart and Horton, 2012; Vacchi et al., 2014). In this database, marine limiting points are typically from samples deposited in the infralittoral zone and from interlaced roots and rhizomes of the marine seagrass *Posidonia oceanica* (known as *matte*, López-Merino et al., 2017). Terrestrial limiting points are typically samples deposited in freshwater swamps, fluvial environments and upper beach/foreshore deposits (Table 1). Furthermore, we considered terrestrial limiting points those archaeological indicators that were theoretically above the MSL at the time of their functioning period, such as tombs and burials (Auriemma and Solinas, 2009).

#### 4.2. Altitude of the RSL data points

For each dated SLIP, RSL is estimated by the following equation:

$$RSL_i = A_i - RWL_i \quad (1)$$

(Shennan and Horton, 2002), where  $A_i$  is the altitude and  $RWL_i$  is the reference water level of sample  $i$ , both expressed relative to the

same datum; i.e. MSL in our analysis.

The total vertical uncertainty on  $RSL_i$  is mainly represented by the indicative range and by the elevation error (Shennan and Horton, 2002). In the database presented here, the latter range from  $\pm 0.05$  m for sample altitudes measured using high-precision survey methods (e.g., differential GPS) to  $\pm 0.5$  m when the altitude was estimated using Digital Elevation Models, such as the sites of Torregrande and Posada in Sardinia (Melis et al., 2017, 2018).

In line with Hijma et al. (2015), we also considered and corrected for the following potential sources of additional vertical uncertainties: (1) a core stretching/shortening error ( $\pm 0.15$  m for rotary corers and vibracores to  $\pm 0.05$  m for hand coring), (2) a sample thickness uncertainty (3) an angle of borehole uncertainty, as a function of the overburden of the sample, taken in this study to be 1%, and (4) an environmental uncertainty of 0.5 m for those samples deposited in undifferentiated brackish environments (Vacchi et al., 2016, see section 4.1). Due to the microtidal setting of the research area and lack of specific regional studies, we did not include an uncertainty term for potential changes in the palaeo-tidal range.

We subdivided the SLIPs into intercalated and basal categories (Horton and Shennan, 2009). Intercalated samples are those recovered from organic horizons located between clastic layers and, therefore, are subject to compaction (e.g., Hijma et al., 2015). Basal lagoonal samples are recovered from sedimentary units overlying incompressible substrates (rocky basements or a thick layer of coarse sand or gravel) and are therefore less prone to compaction. Virtually incompressible samples are also the fossil

remains of fixed biological indicators, represented by fossil rims of *Lithophyllum byssoides* (Laborel et al., 1994; Vacchi et al., 2016) and beachrock samples (Mauz et al., 2015).

#### 4.3. Chronology of sea-level data points

The age of the samples was estimated using radiocarbon ( $^{14}\text{C}$ ) dating of peat layers, organic material, wood, plant remains, sea-grass remains and marine shells. Radiocarbon ages were calibrated into sidereal years with a  $2\sigma$  range. All SLIPs are presented as calibrated years before present (BP), where year 0 is 1950 CE (Stuiver and Polach, 1977) and were calibrated using CALIB 7.1. We employed the IntCal13 and Marine13 (Reimer et al., 2013) datasets for terrestrial and marine samples, respectively. Where available, local reservoir corrections were taken from either the Marine Reservoir Database (Reimer and Reimer, 2001) or from other published values. In calibrating the samples of organic sediment, we assumed that the original depositional environment was a transitional zone in the back-coastal area, influenced by fluvial processes as well as marine inputs. Therefore, for sediment dates where the percentage of marine carbon was available (Melis et al., 2017, 2018) a mixed IntCal13/Marine13 calibration method was applied (Di Rita et al., 2011; Di Rita and Melis, 2013).

A concern with old radiocarbon ages is the correction for isotopic fractionation (Tornqvist et al., 2015) that became a standard procedure at most laboratories by the mid-1980s (Hijma et al., 2015). In the database, the majority of samples were dated after 1990 and, therefore, most are not subject to this potential source of error. For the seven ages that are affected, we followed the procedure described by Hijma et al. (2015) to correct for isotopic fractionation.

## 5. Prediction of RSL

The RSL calculations presented herein have been performed using the Sea Level Equation solver SELEN (<https://geodynamics.org/cig/software/selen/>). The program, which was first introduced by Spada and Stocchi (2007) adopting the classical GIA theory of Farrell and Clark (1976), has now been improved and includes the rotational feedbacks on sea level, according to the method outlined by Milne and Mitrovica (1998). Furthermore, following the generalised Sea Level Equation theory described by Mitrovica and Milne (2003), our calculations fully account for the horizontal migration of the shorelines, for the transition from grounded to floating ice and for time variations of the ocean function in response to sea-level variations. In our GIA runs, we adopted the recent ICE-6G\_C chronology (Peltier et al., 2015), and the mantle rheological profile VM5a. The Sea Level Equation is solved to harmonic degree 256, on a global equal area grid with spacing of  $\sim 20$  km.

## 6. Results

We assessed 169 new radiocarbon-dated RSL data points collected in the western Mediterranean Sea. We combined these new data with 78 RSL data reported in Vacchi et al. (2016). We then reconstructed the RSL histories of the 5 regions using a database comprising 165 SLIPs and 70 limiting points (appendix A). 12 data points were rejected because of i) dating problems (i.e., Bonifacio Strait beachrocks, Vacchi et al., 2017) and anomalous  $\delta^{13}\text{C}$  (‰) values of the sample, ii) difficulties in the definition of the indicative meaning and iii) discrepancies in the measurements of the altitude of archaeological structures.

The newly produced RSL data points (162 SLIPs and limiting points) constitute  $\sim 68\%$  of the present database; the number of SLIPs (Fig. 2A) was increased by  $\sim 58\%$  with respect to the Vacchi

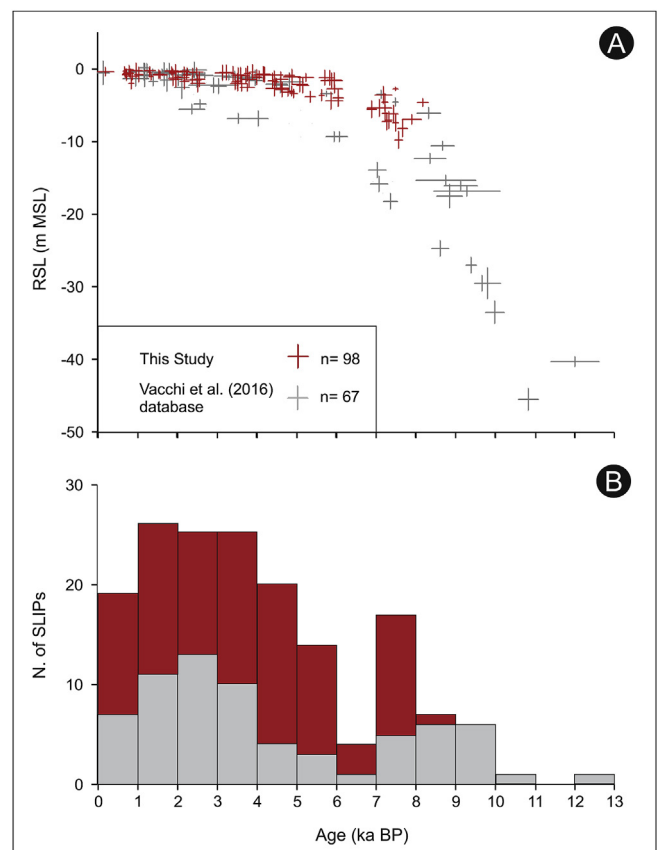


**Fig. 2.** A) Total plot of the 165 SLIPs used for the RSL reconstructions in the 5 regions. Red SLIPs represent those produced for the present database. Grey SLIPs are those included in the Vacchi et al. (2016) compilation. B) Stacked histogram of the SLIPs showing an increase in the number of SLIPs compared to the Vacchi et al. (2016) compilation. (For interpretation of the references to colour in this figure legend, the reader is referred to the Web version of this article.)

et al. (2016) compilation. It has engendered a significant improvement in the assessment of the RSL histories of the Western Mediterranean. The age range of the new data spans the last  $\sim 12.0$  ka BP (Fig. 2A), with a considerable increase in the number of SLIPs, notably for the mid to late-Holocene (Fig. 2B).

### 6.1. Catalonia coast (region 1)

In region 1, we improved the RSL history with 15 SLIPs and 19 terrestrial limiting points spanning the last  $\sim 6$  ka BP (Fig. 3). These data, coupled with the previously available SLIPs, facilitate the reconstruction of the RSL history for the last  $\sim 6$  ka BP. A suite of early-Holocene SLIPs documents a rapid rise in RSL from  $-40 \pm 0.8$  m at  $\sim 12.0$  ka BP to  $-12.3 \pm 0.7$  m  $\sim 8.4$  ka BP. In the mid-Holocene, there is a significant discrepancy between the new data and some of the older SLIPs (Fig. 3). However, two basal SLIPs robustly place the RSL position at  $\sim -3.0$  m at  $\sim 5.8$  ka BP. RSL rose slowly to  $-2.6 \pm 0.5$  m at  $\sim 4.6$  ka BP and at  $-0.8 \pm 0.6$  m at  $\sim 2.0$  ka BP. In the last 1.5 ka BP the total RSL variation was  $-0.1 \pm 0.6$  m.

### 6.2. Balearic Islands (region 2)

The RSL record for region 2 includes 27 SLIPs and 7 limiting points (Fig. 3). They constrain  $\sim 9.5$  ka BP of RSL evolution in an area lacking any previous sea-level reconstructions. A suite of marine limiting points constrains the RSL to above  $\sim -21$  m at  $\sim 9.5$  ka BP,

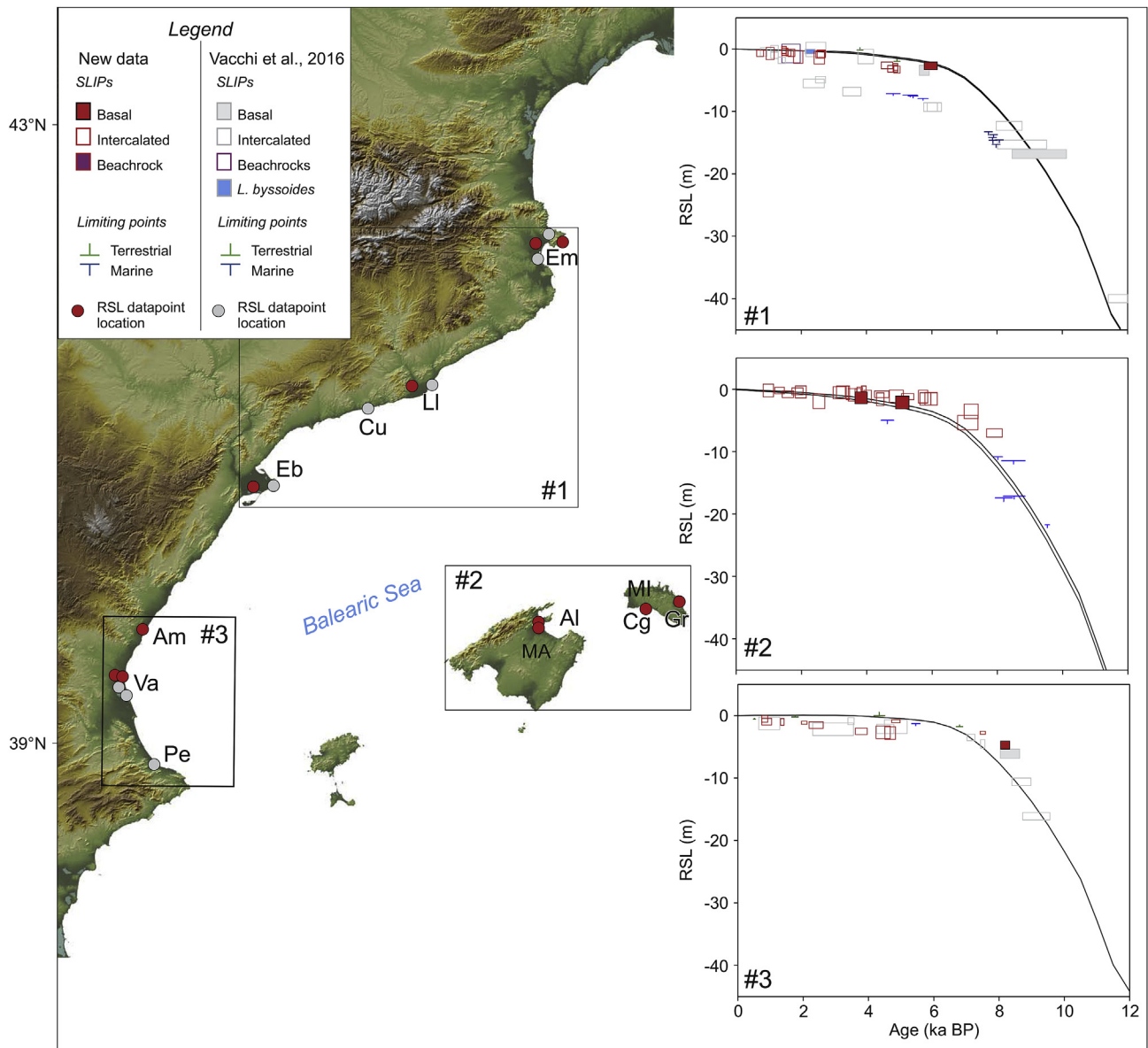


**Fig. 3.** RSL reconstructions in Catalonia (1), the Balearic Islands (2) and Gulf of Valencia (3) regions. The dimensions of boxes (SLIPs) and lines (limiting points) are based on elevation and age errors. Black lines denote the geography of relative sea-level predictions calculated using SELEN and adopting the ICE-6G (VM5a) GIA model (see section 5). Pe: Pego; Va: Valencia; Am: Amenara; Ed: Ebro Delta; Cu: Cubelles; LI: Llobregat Delta; Em: Empuries; AI: Alcudia; Gr: El Grau.

above  $\sim -11.5$  m at  $\sim 8.4$  ka BP and above  $\sim -10.8$  m at  $\sim 8.0$  ka BP. The oldest SLIP indicates that RSL was at  $-6.9 \pm 0.8$  m at  $\sim 7.9$  ka BP, followed by a continuous rising rate which brought the RSL to  $-3.6 \pm 0.8$  m at  $\sim 7.2$  ka BP and to  $-1.5 \pm 0.8$  m at  $\sim 6.0$  ka BP when a SLIP places RSL at  $-1.5 \pm 0.8$  m. Since that period, the rising trend has slowed dramatically, with total RSL variation being within 1.7 m during the last 5.3 ka BP. Younger SLIPs place the RSL at  $-0.5 \pm 1$  m at  $\sim 3.5$  ka BP and at  $-0.4 \pm 1$  m at  $\sim 2.0$  ka BP.

### 6.3. Gulf of Valencia (region 3)

In region 3, we improved the RSL record with 11 SLIPs and 5 limiting points spanning the last  $\sim 8.2$  ka BP (Fig. 3). These new data, added to the previously available ones, allow us to assess the RSL history for the last  $\sim 9.1$  ka BP, when the oldest SLIP places the RSL at  $-16.1 \pm 0.6$  m (Fig. 3). RSL rose rapidly to  $-10.6 \pm 0.6$  m at  $\sim 8.7$  ka BP, to  $-4.6 \pm 0.5$  m at  $\sim 8.2$  ka BP and to  $-2.1 \pm 0.3$  m at  $\sim 7.5$  ka BP.

Despite significant scatter, younger RSL data clearly show a significant deceleration in the rising trend. At  $\sim 4.8$  ka BP, one SLIP places the RSL at  $-0.9 \pm 0.3$  m while the remaining data are consistent with total RSL variation not exceeding 1 m in the late-Holocene period (Fig. 3).

### 6.4. Corsica Island (region 4)

In region 4, we improved the RSL record with 27 SLIPs and 16 limiting points spanning the last 5.4 ka BP (Fig. 4). These data, merged with the previously available ones, constrain a RSL history that spans the last  $\sim 8.8$  ka BP (Fig. 4). The oldest SLIPs are both beachrocks and document a progressive RSL rise from  $-17.5 \pm 1.6$  m at 8.8 ka BP to  $-3.8 \pm 0.8$  m at  $\sim 5.4$  ka BP. One younger lagoonal SLIP places the RSL at  $-1.4 \pm 1.0$  m at  $\sim 4.6$  ka BP. Since this period, the RSL is robustly constrained with the new SLIPs (mainly from lagoonal samples) that are in very good agreement



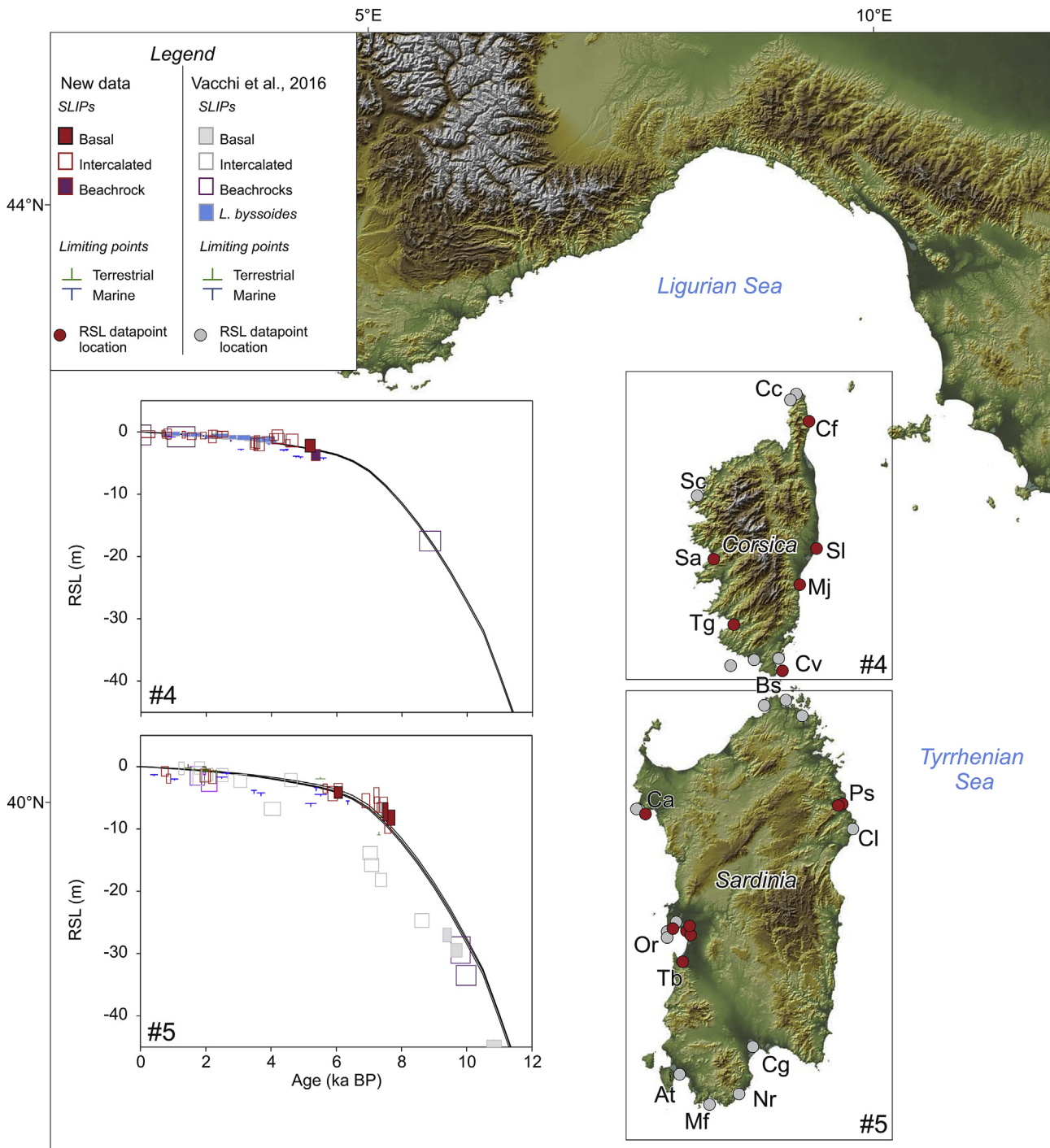


**Fig. 4.** RSL reconstructions in northern Corsica (4) and Sardinia (5) regions. The dimensions of boxes (SLIPs) and lines (limiting points) are based on elevation and age errors. Black lines denote the geography of relative sea-level predictions calculated using SELEN and adopting the ICE-6G (VM5a) GIA model (see section 5). Cc: Cap Corse; Cf: Cala Francese; Sc: Scandola; SI: Sale lagoon; Sa: Sagone; Tg: Tanghiccìa; Cv: Cavallo Island; Bs: Bonifacio Strait; Mj: Mignataghja; Ps: Posada; Ca: Capo Caccia; Cl: Cala Liberotto; Or: Gulf of Oristano; Tb: Terralba; At: Sant’Antioco; Mf: Capo Malfatano-Piscinni; Nr: Nora; Cg: Cagliari.

with the previously available *Lithophyllum byssoides* SLIPs. At ~4.5 and 3.5 ka BP, RSL was at  $-1.8 \pm 0.5$  and  $-1.1 \pm 0.3$  m, respectively. RSL rose slowly to  $-0.8 \pm 0.3$  m at ~2.1 ka BP and the total RSL variation in the last ~1.6 ka BP was within ~0.7 m.

6.5. Sardinia Island (region 5)

In region 5, we improved the RSL record with 17 SLIPs and 18

limiting points spanning the last ~7.7 ka BP. These data, coupled with previously available ones, shed new light on a RSL history covering the last ~11 ka BP (Fig. 4). A suite of basal and beachrocks SLIPs documents the rapid RSL rise of the early-Holocene from  $-45.5 \pm 1.6$  m at ~10.8 ka BP to  $-27 \pm 1.1$  m at ~9.4 ka BP. At the beginning of the mid-Holocene, two basal SLIPs place the RSL at  $-8.2 \pm 1.2$  and at  $-7.4 \pm 1.2$  m at ~7.7 and ~7.5 ka BP, respectively. These data are only partly in agreement with two terrestrial

limiting points derived from Neolithic burials (~7.3 ka BP) found in the Grotta Verde cave. In fact, a first limiting point constrains the RSL below ~-8 m while a second one constrains the RSL ~2 m deeper (below -10 m, Fig. 4). The subsequent mid-Holocene RSL evolution is constrained by a suite of SLIPs placing RSL at  $-4.4 \pm 0.8$  m at ~6.0 ka BP, at  $-3.6 \pm 0.8$  m at ~5.6 ka BP and finally at  $-2.2 \pm 1.1$  m at ~4.6 ka BP. The new mid-Holocene dataset shows significant discrepancy with respect to the previously available SLIPs, mainly represented by the lagoonal samples from the Gulf of Cagliari and the beachrocks found in the northern sector of the Island (Fig. 4).

The late-Holocene record shows significant scatter, mainly related to the large error bar of most of the SLIPs. A SLIP places the RSL at  $-2.3 \pm 1.0$  m at ~3.1 ka BP. At ~2.6 ka, a marine limiting point constrains the RSL above  $-1.1 \pm 0.2$  m, in agreement with a slightly younger (~2.5 ka BP) SLIP that places the RSL at  $-1.4 \pm 1.0$  m. At ~2.0 ka BP, archaeological RSL datapoints (SLIPs and terrestrial) constrain the RSL to between -0.6 and -1.4 m while a younger SLIP places the RSL at  $-0.3 \pm 1.1$  m at ~1.3 ka BP.

## 7. Discussion

The main result of our work is a new compilation of RSL data that significantly improves the reconstruction of RSL histories for five Western Mediterranean regions that were previously characterized by either a paucity of data or conflicting records (Vacchi et al., 2016). The newly assembled database therefore constitutes an essential benchmark to evaluate RSL patterns in the western Mediterranean Sea.

In effect, sediment compaction significantly influenced previous RSL reconstructions, such as those recorded in the Ebro and Llobregat deltas (Somoza et al., 1998; Gámez Torrent, 2007) and the Cagliari coastal plain (Orrù et al., 2004; Antonioli et al., 2007). Moreover, dating problems associated with old beachrock samples from sites located between Corsica and Sardinia (Fig. 4, Bonifacio Strait, Nesteroff, 1984; De Muro and Orrù, 1998) led to poor constraints on RSL evolution, notably for the mid to late-Holocene (Vacchi et al., 2017).

The newly assembled RSL record clearly shows a rapid rise in the early-Holocene (~12.0 to ~8.0 ka BP) followed by a sudden slowdown in the rates of RSL rise in the mid-Holocene (~7.5 and ~4.0 ka BP) and, finally, by minimal changes during the late-Holocene (since ~4.0 ka BP). This sudden reduction in the rising rates closely mirrors the final phase of the North America deglaciation (~7.0 ka BP; Lambeck et al., 2014). This Holocene sea-level behaviour is in agreement with the pattern previously reported along the tectonically stable coasts of the Western Mediterranean (Vacchi et al., 2016).

The new record from Catalonia shows agreement with the ICE-6G (VM5a) GIA model and is comparable, within errors, to the reconstructed RSL histories of the French Mediterranean coast and northwest Italy (Vacchi et al., 2016). This suggests minimal variations in the isostatic pattern over much of the northern coast of the western Mediterranean.

Similarly, the ICE-6G (VM5a) model shows agreement with the data from Corsica and Sardinia, where the expanded RSL record allowed us to resolve conflicting data and to improve our ability to quantify the maximum isostatic contribution in the western Mediterranean basin by very significantly increasing the number of SLIPs for the last ~8.0 ka BP (see details in section 7.1).

By contrast, the model underestimates the RSL position in both the Gulf of Valencia and in the Balearic Islands, especially for the mid-Holocene. However, the RSL record from Valencia cannot be considered as an ideal setting for testing GIA models, because the area is potentially affected by land-level changes related to

historical seismicity (Olivera et al., 1992; Anzidei et al., 2014). Moreover, GPS vertical velocities document a general subsidence trend ( $\leq 2 \text{ mm a}^{-1}$ ), especially for the Valencia coastal plains (Serpelloni et al., 2013), where most of the data were collected. For this reason, the RSL record from Valencia should be used with caution because post-depositional vertical changes (either positive or negative) may have affected the current elevation of the SLIPs and limiting points.

The Balearic Islands are located far from the Mediterranean's major tectonic boundaries (Faccenna et al., 2014; Devoti et al., 2017) and have been affected by negligible historical seismicity (Nocquet, 2012) and by minimal vertical motions during the last ~125 ka BP (Dorale et al., 2010; Stocchi et al., 2018). Here, the fit between the ICE-6G (VM5a) GIA model and the geological RSL data does not appear to be completely satisfactory, especially with regards to the mid-Holocene. This raises intriguing questions and issues potentially related to GIA processes that we address in section 7.2.

### 7.1. New insights into the RSL evolution of Corsica and Sardinia

A variety of geophysical models (Lambeck and Purcell, 2005; Stocchi and Spada, 2007; Roy and Peltier, 2018) predict maximum GIA-related subsidence in the centre of the western Mediterranean basin and notably along the coasts of Sardinia. This assumption was questioned by Pirazzoli (2005), who, for the last two millennia, suggested a general overestimation of the predicted isostatic signal in this area. In a more recent analysis, Antonioli et al. (2007) and subsequently Lambeck et al. (2011) improved the knowledge of the RSL evolution of Sardinia by combining previously available data (Lambeck et al., 2004) with a number of archaeological RSL indicators spanning the last 2.5 ka.

These coastal archaeological structures, mainly comprising coastal quarries, harbour structures and tombs provided new points to reconstruct the RSL history of Sardinia, representing a minimal limit for the RSL position (i.e., terrestrial limiting points, Auriemma and Solinas, 2009; Morhange and Marriner, 2015). These data, coupled with the new SLIPs included in the present database are not consistent with a negligible RSL variation in the last 2.0 ka BP as suggested by Pirazzoli (2005). Specifically, they are consistent with a RSL change greater than ~0.8 m in the last ~2.3 ka BP (Phoenician tomb found at ~-0.76 m MSL; Antonioli et al., 2007). Unfortunately, the large vertical uncertainties of the new Sardinian SLIPs do not help to significantly improve the quality of the late-Holocene RSL history.

Conversely, the new dataset for Corsica robustly corroborates the previous RSL reconstructions (Laborel et al., 1994; Vacchi et al., 2017), with an entire RSL variation that has not exceeded ~1.5 m since the beginning of the late-Holocene. During this period (e.g., last ~4.0 ka BP), any RSL change in tectonically stable regions is entirely controlled by GIA-related subsidence (e.g., Milne et al., 2005; Engelhart et al., 2009). The new dataset for Corsica suggests a relatively uniform GIA-related subsidence pattern for the whole island, with rates of ~0.4 mm a<sup>-1</sup> during the last 4.0 ka. Even if the magnitudes are different, current GIA models (e.g., Stocchi and Spada, 2009; Lambeck et al., 2011; Roy and Peltier, 2018) predict an increase in GIA subsidence rates from Corsica to Sardinia. Unfortunately, the lack of robust SLIPs for Sardinia during the last 4.0 ka BP hampers a proper assessment of this assumption, and additional investigations are therefore required to improve understanding of the local late-Holocene RSL history.

By contrast, the new dataset for Sardinia has yielded new information to assess the mid-Holocene RSL evolution of the area. As stated in the introduction, the previously available data were mainly based on lagoonal samples from the Cagliari plain (probably affected by compaction, Antonioli et al., 2007) and on beachrock



samples mostly collected in the Bonifacio strait (Nesteroff, 1984; De Muro and Orrù, 1998), which are potentially affected by apparent younger ages related to problems in the radiometric dating of bulk cement more than 30 years ago (Vacchi et al., 2017). The new lagoonal SLIPs, collected from both the eastern and the western coasts of the island, show a significant departure from the data previously available for the Sardinian coast. In fact, the new dataset is consistent with a RSL variation that did not exceed ~9 m in the last ~7.5 ka BP. This is concomitant with the Neolithic burials (~7.3 ka BP) found at ~-8.5 m in the Grotta Verde cave (Antonioli et al., 1996, 2012; Guillot, 1997), but conflicts with the coeval pottery found in the same cave at -10 to -11 m (Benjamin et al., 2017; Palombo et al., 2017). Exploration of this submerged cave dates back to the 1970s (Lo Schiavo, 1987) and it represents one of the oldest archaeological findings used to infer past sea level in the Mediterranean (Benjamin et al., 2017). However, considerable debris flow is reported along the flank of the cave and several ceramic fragments were found mixed within these debris down to ~-22 m (Guillot, 1997). Furthermore, lack of information on the levelling tools adopted during the cave exploration makes difficult to properly assess the vertical uncertainty of these archaeological findings. The large number of SLIPs produced in this paper seems to suggest that the terrestrial limiting point found at -10 to -11 m may significantly underestimate the RSL position in the first portion of the mid-Holocene. However, new high-resolution mapping of archaeological findings and of the stratigraphic context of the Grotta Verde are imperative to shed fresh light on this important palaeo sea-level position.

## 7.2. The Balearic Islands: an isostatic conundrum

The new dataset from the Balearic Islands is interesting for an assessment of the GIA pattern within the Mediterranean basin. This is because the maximum GIA-related subsidence of the whole Western Mediterranean (with a magnitude comparable to Sardinia)

is predicted in the Balearic region (Lambeck et al., 2004; Lambeck and Purcell, 2005; Stocchi and Spada, 2007; Roy and Peltier, 2018, Fig. 5B). However, comparison with the Sardinia record shows clear discrepancies with the Balearic Islands, with the RSL history in the latter plotting significantly above the first one. For instance, at ~6.0 ka BP, RSL in the Balearic Islands (Fig. 3) was at least ~2 m higher than in Sardinia (Fig. 4).

As already discussed above, the Balearic Islands are considered to be amongst the most tectonically stable areas of the Mediterranean (Fornós et al., 2002; Dorale et al., 2010; Sàbat et al., 2011). Thus, any possible tectonic movement cannot account for the observed discrepancy that is most likely related to a differential GIA response in this Mediterranean sector. The RSL history of this portion of the basin may thus represent **an unicum in the western Mediterranean**, for which the entire RSL variation in the last ~6.0 ka BP is within ~2.5 m. The new lagoonal data are in agreement with the RSL reconstruction proposed on the basis of archaeological findings and submerged speleothems (Gràcia et al., 2003; Tuccimei et al., 2010) and provides evidence that GIA-related subsidence for this sector of the Mediterranean basin was minimal.

In Fig. 5A, we compared the best estimates of RSL changes in the Balearic Islands with Sardinia, both spanning the last ~8.0 ka BP. In these regions, a comparable GIA fingerprint is predicted by the available models (Galassi and Spada, 2014, Fig. 5B).

This comparison suggests a significant offset between the two RSL records, in conflict with the GIA model predictions. Although these data need to be corroborated by additional RSL investigations, we remark that understanding the causes of the departure of the Balearic record with respect to other regions in the database is crucial in refining the geography of isostatic processes in the Mediterranean. This is, in turn, essential in (i) defining future relative sea-level rise scenarios (e.g., Church and White, 2006; Love et al., 2016) and (ii) testing the exportability of global GIA models (e.g., Roy and Peltier, 2018). Concerning the model predictions, it should be noted that the GIA models currently employed to model

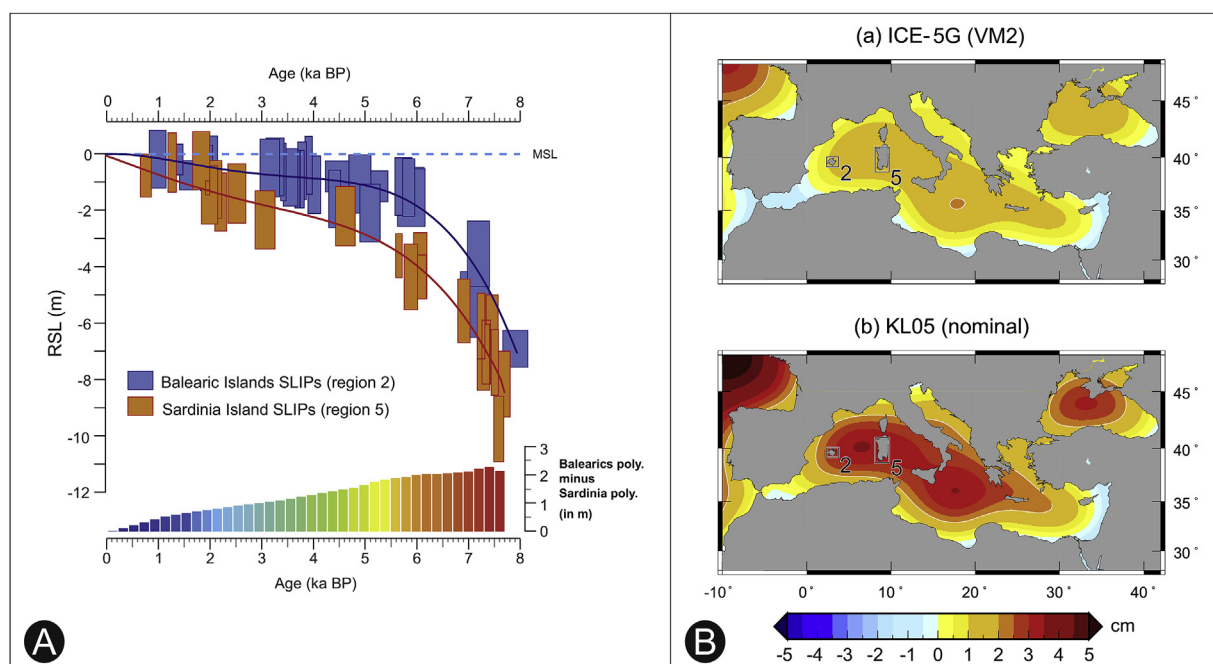


**Fig. 5.** A) Top: 4th-order polynomial fits of the Balearics (blue, region 2) and Sardinia (red, region 5) SLIPs. Bottom: Difference between the two fitted RSL curves through time, in metres. B) GIA sea-level fingerprints for 2040–2050 relative to 1990–2000 in the Mediterranean Sea (modified from Galassi and Spada, 2014). Predictions were obtained by SELEN (Spada and Stocchi, 2007), using models ICE-5G (VM2) (a, Peltier, 2004) and KL05 (b, Lambeck et al., 1998, Lambeck and Purcell, 2005). (For interpretation of the references to colour in this figure legend, the reader is referred to the Web version of this article.)

RSL in the Mediterranean Sea (Lambeck and Purcell, 2005; Stocchi and Spada, 2007, 2009; Roy and Peltier, 2018) are affected by a major limitation since they do not take into account the lateral variations in mantle viscosity or in the thickness of the lithosphere. From global calculations, we know that these may well affect the Earth's response to deglaciation (e.g., Spada et al., 2006).

## 8. Conclusions

In this paper, we produced a new dataset of RSL index and limiting points for a number of Mediterranean regions affected by minimal tectonic influence and where GIA was the major driver of RSL evolution, notably for the last 8000 years. The isostatic pattern defined from newly assembled databases shows significant disparity with respect to those predicted by present GIA models. In particular, the new data outline a non-coherent isostatic response of the central portion of the western Mediterranean, with the Balearic Islands manifesting significant departures from the RSL evolution recorded in Corsica and Sardinia.

The new data presented in this study are crucial in defining the maximum magnitude of the GIA contribution along the Mediterranean coast. Ongoing GIA-related vertical motions represent a key parameter to quantify any possible post-industrial acceleration in RSL rise and to define future scenarios of coastal inundation in the Mediterranean region.

## Acknowledgments

This paper is dedicated to Paolo A. Pirazzoli (1939–2017), a pioneer of sea-level research in the Mediterranean Sea. Our study is a contribution to the MOPP-Medflood (INQUA CMP 1603P) and HOLSEA (INQUA CMP 1601P) projects. Thanks are also due to the PALSEA 2 (PAGES/INQUA/WUN working group) and IGCP Project 639 communities for the fruitful discussions during the workshops. This study was funded by the CNRS MISTRAL PALEOMEX INEE and by the DRAC Corsica. This work was also supported by the Institutional Strategy of the University of Bremen, funded by the German Excellence Initiative (ABPZuK-03/2014) and by ZMT, the Centre for Tropical Marine Ecology. GS is funded by FFABR (Finanziamento delle Attività Base di Ricerca) grant of MIUR (Ministero dell'Istruzione dell'Università e della Ricerca). CM and MV contribute to the Labex OT-Med (ANR-11-LABX-0061) and to the Labex Archimede (ANR-11-LABX-0031-01). MG was supported by a University of Durham Junior research fellowship cofunded by the European Union (grant n. 609412). Finally, we thank the two anonymous reviewers for their constructive comments that significantly improved the paper.

## Appendix A. Supplementary data

SLIPs and limiting points included in the Relative Sea Level database. Latitude and Longitude are expressed in decimal degrees.

Supplementary data to this article can be found online at <https://doi.org/10.1016/j.quascirev.2018.10.025>.

## References

Amorosi, A., Colalongo, M.L., Fusco, F., Pasini, G., Fiorini, F., 1999. Glacio-eustatic control of continental–shallow marine cyclicity from late Quaternary deposits of the southeastern Po Plain, northern Italy. *Quat. Res.* 52 (1), 1–13.

Amorosi, A., Bini, M., Giacomelli, S., Pappalardo, M., Ribecai, C., Rossi, V., Sammartino, I., Sarti, G., 2013. Middle to late Holocene environmental evolution of the Pisa coastal plain (Tuscany, Italy) and early human settlements. *Quat. Int.* 303, 93–106.

Antonioli, F., Ferranti, L., Lo Schiavo, F., 1996. The submerged neolithic burials of the grotta Verde at Capo Caccia (Sardinia, Italy) implication for the Holocene sea-level rise. *Memorie Descrittive del Servizio Geologico Nazionale* 52, 290–312.

Antonioli, F., Anzidei, M., Lambeck, K., Auriemma, R., Gaddi, D., Furlani, S., Orru, P., Solinas, E., Gaspari, A., Karinja, S., Kovacic, V., Surace, L., 2007. Sea-level change during the Holocene in Sardinia and in the northeastern Adriatic (central Mediterranean Sea) from archaeological and geomorphological data. *Quat. Sci. Rev.* 26 (19), 2463–2486.

Antonioli, F., Ferranti, L., Fontana, A., Amorosi, A., Bondesan, A., Braitenberg, C., Dutton, A., Fontolan, G., Furlani, S., Lambeck, K., Mastronuzzi, G., Monaco, C., Spada, G., Stocchi, P., 2009. Holocene relative sea-level changes and vertical movements along the Italian and Istrian coastlines. *Quat. Int.* 206 (1), 102–133.

Antonioli, F., Orrù, P., Porqueddu, A., Solinas, E., 2012. Variazioni del livello marino in Sardegna durante gli ultimi millenni sulla base di indicatori geo-archeologici costieri. *L'Africa romana XIX*, pp. 2963–2972. Sassari 2010, Roma 2012.

Anzidei, M., Lambeck, K., Antonioli, F., Furlani, S., Mastronuzzi, G., Serpelloni, E., Vannucci, G., 2014. Coastal structure, sea-level changes and vertical motion of the land in the Mediterranean. *Geol. Soc. Lond. Spec. Publ.* 388 (1), 453–479.

Auriemma, R., Solinas, E., 2009. Archaeological remains as sea level change markers: a review. *Quat. Int.* 206 (1), 134–146.

Benjamin, J., Rovere, A., Fontana, A., Furlani, S., Vacchi, M., Inglis, R.H., Galili, E., Antonioli, F., Sivan, D., Miko, S., Mourtzas, N., Felja, I., Meredith-Williams, M., Goodman-Tchernov, B., Kolaiti, E., Anzidei, M., Gehrels, R., 2017. Late Quaternary sea-level changes and early human societies in the central and eastern Mediterranean Basin: an interdisciplinary review. *Quat. Int.* 449, 29–57.

Billi, A., Faccenna, C., Bellier, O., Minelli, L., Neri, G., Piromallo, C., Presti, D., Scrocca, D., Serpelloni, E., 2011. Recent tectonic reorganization of the Nubia-Eurasia convergent boundary heading for the closure of the western Mediterranean. *Bull. Soc. Geol. Fr.* 182 (4), 279–303.

Blázquez, A.M., Rodríguez-Pérez, A., Torres, T., Ortiz, J.E., 2017. Evidence for Holocene sea level and climate change from Almenara marsh (western Mediterranean). *Quat. Res.* 88 (2), 206–222.

Bonaduce, A., Pinardi, N., Oddo, P., Spada, G., Larnicol, G., 2016. Sea-level variability in the Mediterranean Sea from altimetry and tide gauges. *Clim. Dynam.* 47 (9–10), 2851–2866.

Bradley, S.L., Milne, G.A., Horton, B.P., Zong, Y., 2016. Modelling sea level data from China and Malay-Thailand to estimate Holocene ice-volume equivalent sea level change. *Quat. Sci. Rev.* 137, 54–68.

Burjachs, F., Pérez-Obiol, R., Picornell-Gelabert, L., Revelles, J., Servera-Vives, G., Expósito, I., Yll, E.I., 2017. Overview of environmental changes and human colonization in the Balearic Islands (Western Mediterranean) and their impacts on vegetation composition during the Holocene. *J. Archaeol. Sci.: Report* 12, 845–859.

Caldara, M., Simone, O., 2005. Coastal changes in the eastern tavoliere plain (Apulia, Italy) during the late Holocene: natural or anthropic? *Quat. Sci. Rev.* 24 (18–19), 2137–2145.

Carboni, M.G., Bergamin, L., Di Bella, L., Iamundo, F., Pugliese, N., 2002. Palaeoecological evidences from foraminifers and ostracods on Late Quaternary sea-level changes in the Ombrone river plain (central Tyrrhenian coast, Italy). *Geobios* 35, 40–50.

Carmona, P., Ruiz-Pérez, J.M., Blázquez, A.M., López-Belzunce, M., Riera, S., Orengo, H., 2016. Environmental evolution and mid–late Holocene climate events in the Valencia lagoon (Mediterranean coast of Spain). *Holocene* 26 (11), 1750–1765.

Cazenave, A., Dieng, H.B., Meyssignac, B., Von Schuckmann, K., Decharme, B., Berthier, E., 2014. The rate of sea-level rise. *Nat. Clim. Change* 4 (5), 358–361.

Cearreta, A., Benito, X., Ibáñez, C., Trobajo, R., Giosan, L., 2016. Holocene palaeoenvironmental evolution of the Ebro Delta (Western Mediterranean Sea): evidence for an early construction based on the benthic foraminiferal record. *Holocene* 26 (9), 1438–1456.

Church, J.A., White, N.J., 2006. A 20th century acceleration in global sea-level rise. *Geophys. Res. Lett.* 33 (1).

Curás, A., Ghilardi, M., Peche-Quilichini, K., Fagel, N., Vacchi, M., Delanghe, D., Contreras, D., Vella, C., Ottaviani, J.C., 2017. Reconstructing past landscapes of the eastern plain of Corsica (NW Mediterranean) during the last 6000 years based on molluscan, sedimentological and palynological analyses. *J. Archaeol. Sci.: Report* 12, 755–769.

Daura, J., Sanz, M., Ramos, J., Riera, S., Miras, Y., Allué, E., Picornell-Gelabert, L., López-Reyes, D., Albert, R.M., Macià, L., Domènech, R., Martinell, J., Fornós, J.J., Julià, R., 2016. Palaeoenvironmental record of the Cal Maurici wetland sediment archive in Barcelona (NE Iberian Peninsula) between c. 6000 and 4000 cal. yr BP. *Holocene* 26 (7), 1020–1039.

De Falco, G., Antonioli, F., Fontolan, G., Presti, V.L., Simeone, S., Tonielli, R., 2015. Early cementation and accommodation space dictate the evolution of an overstepping barrier system during the Holocene. *Mar. Geol.* 369, 52–66.

De Muro, S., Orrù, P., 1998. Il contributo delle Beach-Rock nello studio della risalita del mare olocenico. Le Beach-Rock post-glaciali della Sardegna nord-orientale. *Il Quat.* 11 (1), 19–39.

Devoti, R., D'Agostino, N., Serpelloni, E., Pietrantoni, G., Riguzzi, F., Avallone, A., Cavaliere, A., Cheloni, D., Cecere, G., D'Ambrosio, G., Franco, L., Selvaggi, G., Metois, M., Esposito, A., Sepe, V., Galvani, A., Anzidei, M., 2017. A combined velocity field of the mediterranean region. *Ann. Geophys.* 60 (2), 0215.

Di Rita, F., Melis, R.T., 2013. The cultural landscape near the ancient city of Tharros (central West Sardinia): vegetation changes and human impact. *J. Archaeol. Sci.* 40 (12), 4271–4282.

Di Rita, F., Simone, O., Caldara, M., Gehrels, W.R., Magri, D., 2011. Holocene environmental changes in the coastal Tavoliere Plain (Apulia, southern Italy): a multiproxy approach. *Palaeogeogr. Palaeoclimatol. Palaeoecol.* 310 (3), 139–151.

- Dorale, J.A., Onac, B.P., Fornós, J.J., Ginés, J., Ginés, A., Tuccimei, P., Peate, D.W., 2010. Sea-level highstand 81,000 years ago in Mallorca. *Science* 327 (5967), 860–863.
- Dutton, A., Webster, J.M., Zwart, D., Lambeck, K., Wohlfarth, B., 2015. Tropical tales of polar ice: evidence of Last Interglacial polar ice sheet retreat recorded by fossil reefs of the granitic Seychelles islands. *Quat. Sci. Rev.* 107, 182–196.
- Edwards, R., Gehrels, W.R., Brooks, A., Fyfe, R., Pullen, K., Kuchar, J., Craven, K., 2017. Resolving discrepancies between field and modelled relative sea-level data: lessons from western Ireland. *J. Quat. Sci.* 32 (7), 957–975.
- Ejarque, A., Julia, R., Reed, J.M., Mesquita-Joanes, F., Marco-Barba, J., Riera, S., 2016. Coastal evolution in a Mediterranean microtidal zone: mid to Late Holocene natural dynamics and human management of the Castelló lagoon, NE Spain. *PLoS One* 11 (5), e0155446.
- Engelhart, S.E., Horton, B.P., 2012. Holocene sea level database for the Atlantic coast of the United States. *Quat. Sci. Rev.* 54, 12–25.
- Engelhart, S.E., Horton, B.P., Douglas, B.C., Peltier, W.R., Törnqvist, T.E., 2009. Spatial variability of late Holocene and 20th century sea-level rise along the Atlantic coast of the United States. *Geology* 37 (12), 1115–1118.
- Engelhart, S.E., Peltier, W.R., Horton, B.P., 2011. Holocene relative sea-level changes and glacial isostatic adjustment of the US Atlantic coast. *Geology* 39 (8), 751–754.
- Engelhart, S.E., Vacchi, M., Horton, B.P., Nelson, A.R., Kopp, R.E., 2015. A sea-level database for the Pacific coast of central North America. *Quat. Sci. Rev.* 113, 78–92.
- Faccenna, C., Becker, T.W., Auer, L., Billi, A., Boschi, L., Brun, J.P., Capitanio, F., Funicello, F., Horvat, F., Jolivet, L., Piromallo, C., Royden, L., Rossetti, F., Serpelloni, E., 2014. Mantle dynamics in the mediterranean. *Rev. Geophys.* 52 (3), 283–332.
- Faivre, S., Bakran-Petricoli, T., Horvatinić, N., Sironić, A., 2013. Distinct phases of relative sea level changes in the central Adriatic during the last 1500 years—influence of climatic variations? *Palaeogeogr. Palaeoclimatol. Palaeoecol.* 369, 163–174.
- Farrell, W., Clark, J., 1976. On postglacial sea-level. *Geophys. J. Roy. Astron. Soc.* 46, 647–667.
- Ferranti, L., Antonioli, F., Anzidei, M., Monaco, C., Stocchi, P., 2010. The timescale and spatial extent of vertical tectonic motions in Italy: insights from relative sea-level changes studies. *J. Virtual Explor.* 36 (Paper 30).
- Ferranti, L., Antonioli, F., Mauz, B., Amorosi, A., Dai Pra, G., Mastronuzzi, G., Monaco, C., Orru, P., Pappalardo, M., Radtke, U., Renda, P., Romano, P., Sanso, P., Verrucchi, V., 2006. Markers of the last interglacial sea-level high stand along the coast of Italy: tectonic implications. *Quat. Int.* 145, 30–54.
- Fontana, A., Vinci, G., Tasca, G., Mozzi, P., Vacchi, M., Bivi, G., Rossatto, S., Salvador, L., Antonioli, F., Asioli, A., Bresolin, M., Di Mario, F., Hajdas, I., 2017. Lagoonal settlements and relative sea level during Bronze Age in Northern Adriatic: geoarchaeological evidence and paleogeographic constraints. *Quat. Int.* 439, 17–36.
- Fornós, J.J., García, M.P.F., Pons, G.X., Pérez, A.B., Fornés, A., Pardo, J.E., Rodríguez-Perea, A., Rosselló, V.M., Segura, F., Servera, J., 1998. Rebliment holocènic a la vall incisa del barranc d'Algardar (Cala Galdana, sud de Menorca, Mediterrània Occidental). *Bolletí de la Societat d'Història Natural de les Balears* 41, 173–189.
- Fornós, J.J., Gelabert, B., Ginés, A., Ginés, J., Tuccimei, P., Vesica, P., 2002. Phreatic overgrowths on speleothems: a useful tool in structural geology in littoral karstic landscapes. The example of eastern Mallorca (Balearic Islands). *Geodin. Acta* 15 (2), 113–125.
- Galassi, G., Spada, G., 2014. Sea-level rise in the Mediterranean Sea by 2050: roles of terrestrial ice melt, steric effects and glacial isostatic adjustment. *Global Planet. Change* 123, 55–66.
- Gámez Torrent, D., 2007. Sequence Stratigraphy as a Tool for Water Resources Management in Alluvial Coastal Aquifers: Application to the Llobregat Delta (Barcelona, Spain). Ph.D Thesis. Technical University of Catalonia, Barcelona, p. 177.
- Gehrels, W.R., Long, A.J., 2007. Quaternary land-ocean interactions: sea-level change, sediments and tsunamis. *Mar. Geol.* 242, 169–190.
- Gehrels, W.R., Dawson, D.A., Shaw, J., Marshall, W.A., 2011. Using Holocene relative sea-level data to inform future sea-level predictions: an example from southwest England. *Global Planet. Change* 78 (3), 116–126.
- Ghilardi, M., Delanghe, D., Demory, F., Leandri, F., Pêche-Quilichini, K., Vacchi, M., Vella, M.A., Rossi, V., Robresco, S., 2017a. Enregistrements d'événements extrêmes et évolution des paysages dans les basses vallées fluviales du Taravo et du Sagone (Corse occidentale, France) au cours de l'âge du Bronze moyen à final: une perspective géoarchéologique. *Géomorphol. Relief, Process. Environ.* 23 (1), 15–35.
- Ghilardi, M., Istria, D., Curràs, A., Vacchi, M., Contreras, D., Vella, C., Dussouillez, P., Crest, Y., Guiter, F., Delanghe, D., 2017b. Reconstructing the landscape evolution and the human occupation of the lower Sagone river (western Corsica, France) from the bronze age to the medieval period. *J. Archaeol. Sci.: Report* 12, 741–754.
- Ghilardi, M., Vacchi, M., Curràs, A., Muller Celka, S., Theurillat, T., Lemos, I., Pavlopoulos, K., 2018. Geoarchaeology of coastal landscape along the south euboean Gulf (Euboea island, Greece, during the Holocene). *Quaternaire* 29 (2), 95–120.
- Giaime, M., Morhange, C., Ontiveros, M.Á.C., Fornós, J.J., Vacchi, M., Marriner, N., 2017. In search of Pollentia's southern harbour: geoarchaeological evidence from the Bay of Alcúdia (Mallorca, Spain). *Palaeogeogr. Palaeoclimatol. Palaeoecol.* 466, 184–201.
- Goldberg, S.L., Lau, H.C., Mitrovica, J.X., Lamy, K., 2016. The timing of the Black Sea flood event: insights from modeling of glacial isostatic adjustment. *Earth Planet. Sci. Lett.* 452, 178–184.
- Gràcia, F., Jaume, D., Ramis, D., Fornós, J.J., Bover, P., Clamor, B., Gual, M.A., Vadell, M., 2003. Les coves de Cala Anguila (Manacor, Mallorca). II: La Cova Genovesa o Cova d'en Bessó. Espeleogènesi, geomorfologia, hidrologia, sedimentologia, fauna, paleontologia, arqueologia i conservació. *Endins* 25, 43–86.
- Guillot, F., 1997. La grotta di Sant elmo o "Grotta Verde" in Alghero. *Rev. Luna Azul* 8 (8), 81–92.
- Hijma, M., Engelhart, S.E., Törnqvist, T.E., Horton, B.P., Hu, P., Hill, D.F., 2015. In: Shennan, I., Long, A.J., Horton, B.P. (Eds.), A Protocol for a Geological Sea-level Database. Handbook of Sea-level Research. Wiley Blackwell, pp. 536–553.
- Horton, B.P., Shennan, I., 2009. Compaction of Holocene strata and the implications for relative sealevel change on the east coast of England. *Geology* 37 (12), 1083–1086.
- Kaniewski, D., Marriner, N., Morhange, C., Vacchi, M., Sarti, G., Rossi, V., Bini, M., Pasquonucci, M., Allinne, C., Otto, T., Luce, F., 2018. Holocene evolution of portus pisanus, the lost harbour of pisa. *Sci. Rep.* 8 (1), 11625.
- Karkani, A., Evelpidou, N., Vacchi, M., Morhange, C., Tsukamoto, S., Frechen, M., Maroukian, H., 2017. Tracking shoreline evolution in central Cyclades (Greece) using beachrocks. *Mar. Geol.* 388, 25–37.
- Karkani, A., Evelpidou, N., Giaime, M., Marriner, N., Maroukian, H., Morhange, C., 2018. Late Holocene palaeogeographical evolution of paroiikia bay (paros island, Greece). *Compt. Rendus Geosci.* 350 (5), 202–211.
- Kemp, A.C., Horton, B.P., Culver, S.J., Corbett, D.R., van de Plassche, O., Gehrels, W.R., Douglas, B.C., Parnell, A.C., 2009. Timing and magnitude of recent accelerated sea-level rise (North Carolina, United States). *Geology* 37 (11), 1035–1038.
- Khan, N.S., Ashe, E., Shaw, T.A., Vacchi, M., Walker, J., Peltier, W.R., Kopp, R.E., Horton, B.P., 2015. Holocene relative sea-level changes from near-, intermediate-, and far-field locations. *Curr. Clim. Change Report.* 1 (4), 247–262.
- Khan, N.S., Ashe, E., Horton, B.P., Dutton, A., Kopp, R.E., Brocard, G., Engelhart, S.E., Hill, F.F., Peltier, W.R., Vane, C.H., Scatena, F.N., 2017. Drivers of Holocene sea-level change in the caribbean. *Quat. Sci. Rev.* 155, 13–36.
- Kopp, R.E., Simons, F.J., Mitrovica, J.X., Maloof, A.C., Oppenheimer, M., 2009. Probabilistic assessment of sea level during the last interglacial stage. *Nature* 462 (7275), 863–867.
- Laborel, J., Morhange, C., Lafont, R., Le Campion, J., Laborel-Deguen, F., Sartoretto, S., 1994. Biological evidence of sea-level rise during the last 4500 years on the rocky coasts of continental southwestern France and Corsica. *Mar. Geol.* 120 (3–4), 203–223.
- Lambeck, K., Purcell, A., 2005. Sea-level change in the Mediterranean Sea since the LGM: model predictions for tectonically stable areas. *Quat. Sci. Rev.* 24 (18), 1969–1988.
- Lambeck, K., Smith, C., Johnston, P., 1998. Sea-level change, glacial rebound and mantle viscosity for northern Europe. *Geophys. J. Int.* 134 (1), 102–144.
- Lambeck, K., Antonioli, F., Purcell, A., Silenzi, S., 2004. Sea-level change along the Italian coast for the past 10,000 yr. *Quat. Sci. Rev.* 23 (14), 1567–1598.
- Lambeck, K., Antonioli, F., Anzidei, M., Ferranti, L., Leoni, G., Scicchitano, G., Silenzi, S., 2011. Sea level change along the Italian coast during the Holocene and projections for the future. *Quat. Int.* 232 (1), 250–257.
- Lambeck, K., Rouby, H., Purcell, A., Sun, Y., Sambridge, M., 2014. sea Level and global ice volumes from the last glacial maximum to the Holocene. *Proc. Natl. Acad. Sci. Unit. States Am.* 111 (43), 15296–15303.
- Lo Schiavo, F., 1987. Grotta Verde 1979: un contributo sul neolitico antico della Sardegna. *Atti della XXVI Riunione Scientifica dell'Istituto Italiano di Preistoria e Protostoria*, pp. 845–858.
- Lorscheid, T., Stocchi, P., Casella, E., Gómez-Pujol, L., Vacchi, M., Mann, T., Rovere, A., 2017. Paleo sea-level changes and relative sea-level indicators: precise measurements, indicative meaning and glacial isostatic adjustment perspectives from Mallorca (Western Mediterranean). *Palaeogeogr. Palaeoclimatol. Palaeoecol.* 473, 94–107.
- Love, R., Milne, G.A., Tarasov, L., Engelhart, S.E., Hijma, M.P., Lamy, K., et al., 2016. The contribution of glacial isostatic adjustment to projections of sea-level change along the Atlantic and Gulf coasts of North America. *Earth's Future* 4 (10), 440–464.
- López-Merino, L., Colás-Ruiz, N.R., Adame, M.F., Serrano, O., Martínez Cortizas, A., Mateo, M.A., 2017. A six thousand-year record of climate and land-use change from Mediterranean seagrass mats. *J. Ecol.* 105 (5), 1267–1278.
- Marco-Barba, J., Holmes, J.A., Mesquita-Joanes, F., Miracle, M.R., 2013. The influence of climate and sea-level change on the Holocene evolution of a Mediterranean coastal lagoon: evidence from ostracod palaeoecology and geochemistry. *Geobios* 46 (5), 409–421.
- Marriner, N., Flaux, C., Morhange, C., Kaniewski, D., 2012a. Nile Delta's sinking past: quantifiable links with Holocene compaction and climate-driven changes in sediment supply? *Geology* 40 (12), 1083–1086.
- Marriner, N., Gambin, T., Djamali, M., Morhange, C., Spiteri, M., 2012b. Geoarchaeology of the Burmarrad ria and early Holocene human impacts in western Malta. *Palaeogeogr. Palaeoclimatol. Palaeoecol.* 339, 52–65.
- Marriner, N., Morhange, C., Faivre, S., Flaux, C., Vacchi, M., Miko, S., Dumas, V., Boetto, G., Rossi, I.R., 2014. Post-Roman sea-level changes on Pag Island (Adriatic Sea): dating Croatia's "enigmatic" coastal notch? *Geomorphology* 221, 83–94.
- Mastronuzzi, G., Sansò, P., 2002. Holocene uplift rates and historical rapid sea-level changes at the Gargano promontory, Italy. *J. Quat. Sci.* 17 (5–6), 593–606.
- Mauz, B., Vacchi, M., Green, A., Hoffmann, G., Cooper, A., 2015. Beachrock: a tool for reconstructing relative sea level in the far-field. *Mar. Geol.* 362, 1–16.
- Melis, R.T., Depalmas, A., Di Rita, F., Montis, F., Vacchi, M., 2017. Mid to late Holocene



- environmental changes along the coast of western Sardinia (Mediterranean Sea). *Global Planet. Change* 155, 29–41.
- Melis, R.T., Di Rita, F., French, C., Marriner, N., Montis, F., Serreli, G., Sulas, F., Vacchi, M., 2018. 8000 years of coastal changes on a western Mediterranean island: a multiproxy approach from the Posada plain of Sardinia. *Mar. Geol.* 403, 93–108.
- Milne, G., Mitrovica, J., 1998. Postglacial sea-level change on a rotating Earth. *Geophys. J. Int.* 133 (1), 1–19.
- Milne, G.A., Long, A.J., Bassett, S.E., 2005. Modeling Holocene Relative Sea-level observations from the caribbean and south America. *Quat. Sci. Rev.* 24, 1183–1202.
- Milne, G.A., Gehrels, W.R., Hughes, C.W., Tamisiea, M.E., 2009. Identifying the causes of sea-level change. *Nat. Geosci.* 2 (7), 471–478.
- Mitrovica, J.X., Milne, G.A., 2003. On postglacial sea level: I. General Theory. *Geophys. J. Int.* 154 (2), 253–267.
- Morhange, C., Laborel, J., Hesnard, A., 2001. Changes of relative sea level during the past 5000 years in the ancient harbour of Marseilles, Southern France. *Palaeogeogr. Palaeoclimatol. Palaeoecol.* 166, 319–329.
- Morhange, C., Marriner, N., 2015. Archeological and biological relative sea-level indicators. *Handbook of sea-level research* 146–156.
- Nesteroff, W.D., 1984. Étude de quelques grès de plage du sud de la Corse: datations 14C et implications néotectoniques pour le bloc corso-sarde. *Trav. Maison Orient* 8 (1), 99–111.
- Nicholls, R.J., Hanson, S.E., Lowe, J.A., Warrick, R.A., Lu, X., Long, A.J., 2014. Sea-level scenarios for evaluating coastal impacts. *Wiley Interdisciplinary Reviews: Climate Change* 5 (1), 129–150.
- Nocquet, J.M., 2012. Present-day kinematics of the Mediterranean: a comprehensive overview of GPS results. *Tectonophysics* 579, 220–242.
- Olivera, C., Susagna, T., Roca, A., Goula, X., 1992. Seismicity of the Valencia trough and surrounding areas. *Tectonophysics* 203 (1–4), 99–109.
- Orrù, P.E., Antonioli, F., Lambeck, K., Verrubbi, V., 2004. Holocene Sea-level Change in the Cagliari Coastal Plain (Southern Sardinia, Italy). *Quaternaria Nova*.
- Orrù, P.E., Solinas, E., Puliga, G., Deiana, G., 2011. Palaeo-shorelines of the historic period, Sant'Antioco island, south-western Sardinia (Italy). *Quat. Int.* 232 (1), 71–81.
- Orrù, P.E., Mastronuzzi, G., Deiana, G., Pignatelli, C., Piscitelli, A., Solinas, E., Spanu, P., Zucca, R., 2014. Sea level changes and geoarchaeology between the bay of Capo Malfatano and Piscinnu Bay (SW Sardinia) in the last 4 kys. *Quat. Int.* 336, 180–189.
- Palombo, M.R., Antonioli, F., Presti, V.L., Mannino, M.A., Melis, R.T., Orru, P., Stocchi, P., Talamo, S., Quarta, G., Calcagnile, L., Deiana, G., Altamura, S., 2017. The late Pleistocene to Holocene palaeogeographic evolution of the Porto Conte area: clues for a better understanding of human colonization of Sardinia and faunal dynamics during the last 30 ka. *Quat. Int.* 439, 117–140.
- Pascucci, V., De Falco, G., Del Vais, C., Sanna, I., Melis, R.T., Andreucci, S., 2018. Climate changes and human impact on the Mistras coastal barrier system (W Sardinia, Italy). *Mar. Geol.* 395, 271–284.
- Peltier, W.R., 2004. Global glacial isostasy and the surface of the ice-age Earth: the ICE-5G (VM2) model and GRACE. *Annu. Rev. Earth Planet Sci.* 32, 111–149.
- Peltier, W., Argus, D., Drummond, R., 2015. Space geodesy constrains ice age terminal deglaciation: the global ICE-6G\_C (VM5a) model. *J. Geophys. Res.* B 120 (1), 450–487.
- Pirazzoli, P.A., 2005. A review of possible eustatic, isostatic and tectonic contributions in eight late-Holocene relative sea-level histories from the Mediterranean area. *Quat. Sci. Rev.* 24 (18), 1989–2001.
- Poher, Y., Ponel, P., Médail, F., Andrieu-Ponel, V., Guiter, F., 2017. Holocene environmental history of a small Mediterranean island in response to sea-level changes, climate and human impact. *Palaeogeogr. Palaeoclimatol. Palaeoecol.* 465, 247–263.
- Preuss, H., 1979. Progress in computer evaluation of sea level data within the IGCP project no. 61. In: *Proc. 1978 International Symposium of Coastal Evolution in the Quaternary*, pp. 104–134.
- Primavera, M., Simone, O., Fiorentino, G., Caldara, M., 2011. The palaeoenvironmental study of the Alimini Piccolo lake enables a reconstruction of Holocene sea-level changes in southeast Italy. *Holocene* 21 (4), 553–563.
- Purcell, A., Tregoning, P., Dehecq, A., 2016. An assessment of the ICE6G\_C (VM5a) glacial isostatic adjustment model. *J. Geophys. Res.: Solid Earth* 121 (5), 3939–3950.
- Reimer, P.J., Reimer, R.W., 2001. A marine reservoir correction database and on-line interface. *Radiocarbon* 43 (2A), 461–463.
- Reimer, P.J., Bard, E., Bayliss, A., Beck, J.W., Blackwell, P.G., Ramsey, C.B., et al., 2013. IntCal13 and Marine13 radiocarbon age calibration curves 0–50,000 years cal BP. *Radiocarbon* 55 (4), 1869–1887.
- Rodríguez-Pérez, A., Blázquez, A.M., Guillem, J., Usera, J., 2018. Maximum flood area during MIS 1 in the Almenara marshland (Western Mediterranean): benthic foraminifera and sedimentary record. *Holocene*. <https://doi.org/10.1177/0959683618777069> (in press).
- Roqué Pau, C., Pallí Buxó, L., 1997. Depósitos litorales y variaciones del nivel del mar durante el Holoceno en la Costa Brava (NE de Catalunya). In: *Reunion del Cuaternario Ibérico: Asociación Española para el Estudio del Cuaternario [AEQUA]: 1997: Huelva*, 1997, pp. 178–183.
- Rossi, V., Amorosi, A., Sarti, G., Potenza, M., 2011. Influence of inherited topography on the Holocene sedimentary evolution of coastal systems: an example from Arno coastal plain (Tuscany, Italy). *Geomorphology* 135 (1–2), 117–128.
- Rovere, A., Stocchi, P., Vacchi, M., 2016. Eustatic and relative sea level changes. *Curr. Climate Change Report* 2 (4), 221–231.
- Roy, K., Peltier, W.R., 2018. Relative sea level in the Western Mediterranean basin: a regional test of the ICE-7G\_NA (VM7) model and a constraint on late Holocene Antarctic deglaciation. *Quat. Sci. Rev.* 183, 76–87.
- Ruello, M.R., Cinque, A., Di Donato, V., Molisso, F., Terrasi, F., Ermolli, E.R., 2017. Interplay between sea level rise and tectonics in the Holocene evolution of the St. Eufemia Plain (Calabria, Italy). *J. Coast Conserv.* 21 (6), 903–915.
- Ruiz, J.M., Carmona, P., Gomez-Bellard, C., van Dommelen, P., 2018. Geomorphology and environmental change around the punic sites of the Terralba plain (Oristano Gulf, Sardinia, Italy). *Bol. Geol. Min.* 129 (1–2), 331–351.
- Sabat, F., Gelabert, B., Rodríguez-Perea, A., Giménez, J., 2011. Geological structure and evolution of majorca: implications for the origin of the western mediterranean. *Tectonophysics* 510 (1), 217–238.
- Sabatier, P., Dezileau, L., Colin, C., Briquieu, L., Bouchette, F., Martinez, P., et al., 2012. 7000 years of paleostorm activity in the NW Mediterranean Sea in response to Holocene climate events. *Quat. Res.* 77 (1), 1–11.
- Salel, T., Bruneton, H., Lefèvre, D., 2016. Ostracods and environmental variability in lagoons and deltas along the north-western Mediterranean coast (Gulf of Lions, France and Ebro delta, Spain). *Rev. Micropaleontol.* 59 (4), 425–444.
- Sander, L., Fruergaard, M., Koch, J., Johannessen, P.N., Pejrup, M., 2015. Sedimentary indications and absolute chronology of Holocene relative sea-level changes retrieved from coastal lagoon deposits on Samsø, Denmark. *Boreas* 44 (4), 706–720.
- Sander, L., Hede, M.U., Fruergaard, M., Nielsen, L., Clemmensen, L.B., Kroon, A., Johannessen, P.N., Nielsen, L.H., Pejrup, M., 2016. Coastal lagoons and beach ridges as complementary sedimentary archives for the reconstruction of Holocene relative sea-level changes. *Terra. Nova* 28 (1), 43–49.
- Scicchitano, G., Spampinato, C.R., Ferranti, L., Antonioli, F., Monaco, C., Capano, M., Lubritto, C., 2011. Uplifted Holocene shorelines at Capo Milazzo (NE Sicily, Italy): evidence of co-seismic and steady-state deformation. *Quat. Int.* 232 (1), 201–213.
- Serpelloni, E., Vannucci, G., Pondrelli, S., Argnani, A., Casula, G., Anzidei, M., Baldi, P., Gasperini, P., 2007. Kinematics of the Western Africa-Eurasia plate boundary from focal mechanisms and GPS data. *Geophys. J. Int.* 169 (3), 1180–1200.
- Serpelloni, E., Faccenna, C., Spada, G., Dong, D., Williams, S.D., 2013. Vertical GPS ground motion rates in the Euro-Mediterranean region: new evidence of velocity gradients at different spatial scales along the Nubia-Eurasia plate boundary. *J. Geophys. Res.: Solid Earth* 118 (11), 6003–6024.
- Shaw, T.A., Kirby, J.R., Holgate, S., Tutman, P., Plater, A.J., 2016. Contemporary salt-marsh foraminiferal distribution from the Adriatic coast of Croatia and its potential for sea-level studies. *J. Foraminifer. Res.* 46 (3), 314–332.
- Shennan, I., Horton, B., 2002. Holocene land-and sea-level changes in Great Britain. *J. Quat. Sci.* 17 (5–6), 511–526.
- Shennan, I., Long, A.J., Horton, B.P., 2015. *Handbook of Sea-level Research*. John Wiley & Sons.
- Somoza, L., Barnolas, A., Arasa, A., Maestro, A., Rees, J.G., Hernández-Molina, F.J., 1998. Architectural stacking patterns of the Ebro delta controlled by Holocene high-frequency eustatic fluctuations, delta-lobe switching and subsidence processes. *Sediment. Geol.* 117 (1), 11–32.
- Spada, G., Stocchi, P., 2007. SELEN: a fortran 90 program for solving the “sea level equation”. *Comput. Geosci.* 33 (4), 538–562.
- Spada, G., Antonioli, A., Cianetti, S., Giunchi, C., 2006. Glacial isostatic adjustment and relative sea-level changes: the role of lithospheric and upper mantle heterogeneities in a 3-D spherical Earth. *Geophys. J. Int.* 165 (2), 692–702.
- Stiros, S.C., Laborel, J., Laborel-Deguen, F., Papageorgiou, S., Evin, J., Pirazzoli, P.A., 2000. Seismic coastal uplift in a region of subsidence: Holocene raised shorelines of Samos Island, Aegean Sea, Greece. *Mar. Geol.* 170 (1), 41–58.
- Stocchi, P., Spada, G., 2007. Glacio and hydro-isostasy in the Mediterranean Sea: Clark's zones and role of remote ice sheets. *Ann. Geophys.* 50 (6).
- Stocchi, P., Spada, G., 2009. Influence of glacial isostatic adjustment upon current sea level variations in the Mediterranean. *Tectonophysics* 474 (1), 56–68.
- Stocchi, P., Vacchi, M., Lorscheid, T., de Boer, B., Simms, A.R., van de Wal, R.S., Vermeesen, B.L.A., Pappalardo, M., Rovere, A., 2018. MIS 5e relative sea-level changes in the Mediterranean Sea: contribution of isostatic disequilibrium. *Quat. Sci. Rev.* 185, 122–134.
- Stuiver, M., Polach, H.A., 1977. Reporting 14C data. *Radiocarbon* 19, 355–363.
- Tornqvist, T.E., Rosenheim, B.E., Hu, P., Fernandez, A.B., 2015. Radiocarbon dating and calibration. In: Long, A.J., Horton, B.P., Shennan, I. (Eds.), *Handbook of Sea-level Research*. Wiley, pp. 349–360.
- Tsimplis, M.N., Proctor, R., Flather, R.A., 1995. A two-dimensional tidal model for the Mediterranean Sea. *J. Geophys. Res.: Oceans* 100 (C8), 16223–16239.
- Tuccimei, P., Soligo, M., Ginés, J., Ginés, J., Fornós, J., Kramers, J., Villa, I.M., 2010. Constraining Holocene sea levels using U-Th ages of phreatic overgrowths on speleothems from coastal caves in Mallorca (Western Mediterranean). *Earth Surf. Process. Landforms* 35 (7), 782–790.
- Vacchi, M., Rovere, A., Zouros, N., Desruelles, S., Caron, V., Firpo, M., 2012. Spatial distribution of sea-level markers on Lesbos Island (NE Aegean Sea): evidence of differential relative sea-level changes and the neotectonic implications. *Geomorphology* 159, 50–62.
- Vacchi, M., Rovere, A., Chatzipetros, A., Zouros, N., Firpo, M., 2014. An updated database of Holocene relative sea level changes in NE Aegean Sea. *Quat. Int.* 328, 301–310.
- Vacchi, M., Marriner, N., Morhange, C., Spada, G., Fontana, A., Rovere, A., 2016. Multiproxy assessment of Holocene relative sea-level changes in the western Mediterranean: sea-level variability and improvements in the definition of the

- isostatic signal. *Earth Sci. Rev.* 155, 172–197.
- Vacchi, M., Ghilardi, M., Spada, G., Currás, A., Robresco, S., 2017. New insights into the sea-level evolution in Corsica (NW Mediterranean) since the late Neolithic. *J. Archaeol. Sci.: Report* 12, 782–793.
- van de Plassche, O., 1982. Sea-level change and water-level movements in The Netherlands during the Holocene. *Meded. Rijks Geol. Dienst* 36, 1–93.
- Vella, C., Fleury, T.J., Raccasi, G., Provansal, M., Sabatier, F., Bourcier, M., 2005. Evolution of the rhône delta plain in the Holocene. *Mar. Geol.* 222, 235–265.
- Vernant, P., Fadil, A., Mourabit, T., Ouazar, D., Koulali, A., Davila, J.M., Garate, J., McClusky, S., Reilinger, R., 2010. Geodetic constraints on active tectonics of the Western Mediterranean: implications for the kinematics and dynamics of the Nubia-Eurasia plate boundary zone. *J. Geodyn.* 49 (3), 123–129.
- Yll, R., Pantaleón-Cano, J., Pérez-Obiol, R.P., Roure, J.M., 1999. Cambio climático y transformación del medio durante el Holoceno en las Islas Baleares. *Congres del Neolítico a la Península Ibérica, Saguntum Extra* 2, 45–51.